Paper No. 422. (quote when citing this article)
Eleventh World Conference on Earthquake Engineering
ISBN: 0 08 042822 3

DEVELOPMENT OF AN ACTIVE TMD AND CONTROL ALGORITHMS FOR STRONG EARTHQUAKE EXCITATION —NUMERICAL SIMULATION AND SHAKING TABLE TESTS—

H. Iemura[1], A. Igarashi[1] and I. Katayama[2]

[1]Dept. of Civil Engineering, Kyoto University, Kyoto 606-01, Japan
[2]Tokyo Electric Power Service Co.,Ltd. 3-3, Higashi-Ueno 3-choume, Taito-Ku, Tokyo, 110 Japan

ABSTRACT

In this study, a 4-d.o.f. flexible and lightly damped structural frame model with and without these control devices are tested under earthquake ground motion generated by a shaking table. From the test with an AMD (active mass damper), the variable gain control and the stroke limitation control are found to be effective for a wide range of input intensity. And, the SOTMD (self oscillating tuned mass damper) which is one of the active TMD is newly developed. Then, the efficiency of the two control algorithms is compared. It is found that the SOTMD with the most effective control algorithms needs only 10% of the AMD for the same level of dynamic response reduction.

KEYWORDS

Structures, Dynamic Control, Active, TMD, Algorithms, Variable Gain, Nonlinear Control, Stroke Limitation, Active Pendulum, Experiments

INTRODUCTION

Due to recent development of sensoring and digital control techniques, active and hybrid control methods of dynamic response of structures are developed and some are implemented to buildings and bridges. The merit of active control method is that they are effective for a wide-frequency range and also for transient vibration. However, active control method needs a large amount of external energy supply and also a high level of maintenance. The hybrid control method which consists of both passive and active devices has been proposed utilizing the merits of both passive and active methods and avoiding the demerits of these methods.

In the first part of this paper, the active moving mass damper (AMD, hereafter) with variable control gain and also with the stroke limitation is proposed to generate control force against a wide range of input intensity. The efficiency of the algorithms with variable control gain and the stroke limitation is tested from shaking tests of a 4-d.o.f. flexible and lightly damped structural frame model.

In the latter part of this paper, the new type active tuned mass damper (ATMD) is developed. It is a pendulum, which has the AMD inside, and is called the self oscillating TMD (SOTMD). Then, two control algorithms are applied; one is to enhance the movement of the TMD so that the TMD reduces only the first mode vibration of a structure, the other is to reduce the multi-mode dynamic response of the structure. The efficiency is tested by the shaking table tests.

Experimental Setup

As shown in Fig. 1, a flexible 4-d.o.f. structural frame model is tested on a shaking table. The weight of each story is 34.3 kgf and each story height is 34 cm. Each floor consists of 3 steel plates which have much higher stiffness than the flexible steel column models.
The active mass damper (AMD) consists of an AC servo-motor, a screwed bar, a moving mass weighing 3.5kgf and a tube guide for the horizontal movement of the mass, as shown in Fig.2.

At the time of the AMD control mode, AMD is installed at the top floor of the model as shown in Fig.3(a). At the time of the TMD control mode, the total AMD system is hung from the top floor with their four steel plates as shown in Fig. 3. An air damper is used to add an energy absorbing capacity to the TMD. The optimum tuning ratio and the optimum damping ratio are selected for the design of TMD. At the time of the SOTMD control mode, the active mass is activated in the TMD. Mass ratios of the active mass and the tuned mass to the total structural mass are 2.5% and 6.4%, respectively.

Velocity meters are installed on the shaking table and on each floor of the model. The movement of the moving mass, which generates the force of inertia as the control force, is monitored by a small-size accelerometer attached at the top the mass.

Active Control with Variable Gain

To calculate the control force of AMD and SOTMD, the optimum regulator theory is used as follows. The equation of motion is assumed to be expressed by

$$M\ddot{x}+C\dot{x}+Kx = G\ddot{z}+Du \tag{1}$$

where x is the structural displacement vector, $\ddot{z}$ represents the ground acceleration, u denotes the control force vector. The matrices G and D define the forces acting on the d.o.f., and M, C, K are the mass, damping and stiffness matrices, respectively. Upon defining the state vector of the system y by $y^T = \{x^T, \dot{x}^T\}$, one can express the total energy consisting of structural vibration and control force by

$$J = \int_0^\infty (y^T Q y + u^T R u)\,dt \qquad \text{where} \qquad Q = \begin{bmatrix} K & O \\ O & M \end{bmatrix} \tag{2}$$

Using a weighting matrix R and the minimization criteria, the control force is given by

$$u = F_y x + F_z z \tag{3}$$

where Fy and Fz are feedback and feedforward gains, respectively, and z is a vector representing the ground motion.

If the gain is fixed to a relatively large value, high reduction of dynamic response of a structure is obtained. However, when the input excitation level becomes high, the control force is also increased and will reach to its limit value. To maximize the capacity of the controller, it is preferable to use relatively high gains for low level excitation and low gains for high level excitation.

In this study, five levels of gains are prepared for the variable gain control. The gains are shown in Fig.4 which gives the relationship between the control force and the structural vibration energy. Judging from the calculated control force, velocity and displacement of the moving mass, the most appropriate gains are chosen not to exceed the maximum capacity of the motor (1kgf) and the maximum stroke of the moving mass (10cm). As the input ground motion, the scaled El Centro NS earthquake record obtained during the Imperial Valley earthquake 1940 shown in Fig.5 is adopted. Velocity response of the top story of the model with fixed gain 4, with variable gain and without control are shown in Fig.6(b). The selected gains in time history are plotted in Fig.6(a). It is clearly found that lower gains are selected where the response level is relatively high. In this region, there is not much difference between the variable gain and the fixed gain 4. However, in the region where the response level is relatively low, the high gain (gain 1) is mostly selected to obtain more reduction of response than the fixed gain 4. The Fourier spectra of the velocity response are compared in Fig.6(c) from which the variable gain

control is found to give the higher reduction of the response than the fixed gain.

The time histories and Fourier spectra of the control force with the fixed and the variable gains are shown in Fig.7(a) and (b). The time history of the displacement of the moving mass is plotted in Fig.8. From these figures,it is understood that the capacity of the active mass damper (max 1kgf and 10cm) is efficiently mobilized with the variable gain. The maximum and rms of the displacement of the moving mass with the increasing maximum input acceleration are plotted in Fig.9. It is clearly found that the maximum displacement is controlled not to exceed the displacement limit (10cm) with the variable gain control.

The structural vibration energy with the increasing maximum input acceleration is plotted in Fig.10. When the input acceleration is low, the variable gain is close to the high fixed gain 1. When the input acceleration becomes large, the variable gain is close to the low fixed gain. These results verify that the variable gain control method is performing fairly well.

Nonlinear Control of AMD with Stroke Limitation

In this section, Nonlinear control algorithm of AMD with stroke limitation is proposed and its effectiveness verified is by numerical simulations and experiments.

Basic concept of Control Algorithm and Variable Gain. Following the notations in Fig.11, movement of the auxiliary mass is assumed as

$$\dot{W}(t) = \beta x(t) - \alpha W(t) \tag{4}$$

where, α is the restoring spring constant to keep the neutral position of the auxiliary mass. The variable control gain β is assumed to be given by next equation.

$$\beta(E) = W_{max}\omega_0\sqrt{\frac{k}{2E}} \tag{5}$$

where, Wmax is the maximum allowable maximum stroke of the control actuator, ω_0 is the natural frequency of the structure, E is the summation of kinetic and potential energy of the structure. The relation between β and E is shown in Fig.12, where β is set as the constant value β max in the small energy range. This relation is equivalent to linear and saturated movement of auxiliary mass to the input ground motion, which is shown in Fig.13.

Numerical Simulation. The numerical simulation of a structure is performed with and without the control subjected to the El Central Earthquake Motion. The results are shown in Fig.14, from which saturation control of the auxiliary mass is verified.

Shaking Table Tests. Using the same four storied experimental model, shaking table test is conducted. Tested results are shown in Fig.15(a)~(d). In Fig.15(a), the first mode displacement response is compared, with and without the control. The proposed saturation control is also compared with the linear LQ control. Fig.15(a) and (b) show movement of the auxiliary mass with the saturation control and the conventional linear LQ control. The control force of the saturation and LQ control is also compared in Fig,15(d). Form these results, it is observed that controlled displacement shows similar values between LQ and the saturation control, even though large difference in displacement response of the auxiliary mass is found. With the saturation control, the displacement response of the auxiliary mass is well controlled in the limited range. On the contrary, the displacement by the LQ control shows large fluctuation with large amplitude exceeding the displacement limit.

Control Algorithm of SOTMD

The newly developed SOTMD in this study has the following engineering features. 1) Combination of passive and active devices gives an energy efficient system, 2) The active system can contribute to suppress the non-stationary and higher mode components of the response, 3) Even if

the active system is broken down, the passive system keeps functioning.

To activate the AMD of the SOTMD, the following two control algorithms are adopted. In the first control algorithm, only the main structural part shown in Fig.16(a) is considered in the 2performance function given by Eq.2. In this algorithm, movement of the TMD is amplified by the AMD to reduce the first mode vibration of the structure. In the second control algorithm (control 2), TMD and structural parts shown in Fig.16(b) are considered in the performance function. In this algorithm, the AMD works to reduce the total vibrational energy including higher mode components of the structure. The trade-off curves between control force and structural vibration energy with control algorithm 1 and 2 are plotted in Fig.17 together with 5 levels of gains used for shaking table tests. It is clear that the control 1 gives move efficient reduction of the response than the control 2. The reason is that some part of the control energy is used to reduce the dynamic response of the TMD.

Test Results of the SOTMD

For shaking table tests of the SOTMD, the artificial earthquake ground motion shown in Fig.18 for the medium soil condition recommended in the specification for highway bridges is used.
Velocity response of the top floor of the model with the TMD and the SOTMD is plotted in Fig.19 and 20. From these results, it is found that the SOTMD reduces the response more than the TMD. Especially, the first mode response is reduced fairly well by the control 1, (Fig.20(b)), and both the first and the second mode response are reduced by the control 2.

Figure 21 shows the movement of the TMD relative to the top floor, from which control 1 is found to amplify the TMD action.
Energy efficiency of the control 2 is again confirmed from the trade-off curves of the experiment shown in Fig.22.

Figures 23 and 24 are comparison of the control 1 and 2. Even though first mode response levels are similar, much less control force is needed in the control 1. However, control force of the control 2 in the second mode reduces the second mode response effectively.
Figures 25 and 26 shows comparison of the AMD and the SOTMD. From the many experimental results, the cases which give similar response levels are selected (Fig.25) and the corresponding control forces to the AMD and the SOTMD are compared (Fig.26). It is definitely clear that high energy efficiency can be achieved by the SOTMD.

CONCLUSIONS

Conclusions obtained from this study can be briefly summarized as follows.

1) From the shaking table tests of the structural model with the AMD, the active control with the variable gain and the nonlinear control with the stroke limitation are found to work well to maximize the capacity of the devices of the AMD.
2) The new type of a tuned pendulum with an AMD is developed and named as the self oscillating TMD. High energy efficiency of the SOTMD compared to the AMD is experimentally confirmed.
3) From many experimental results with different control algorithms, it is found that amplifying the TMD of the SOTMD by the AMD to reduce the first mode response of the structural model has the highest energy efficiency.

REFERENCES

Iemura, H., et al (1990). "Comparison of Passive, Active and Hybrid Control Techniques on Earthquake Response of Flexural Structures-Numerical Simulations and Experiments," Proc. U.S.-Italy-Japan Workshop/Symposium on Structural Control and Intelligent Systems, Sorento.

Igarashi, A., et al (1995). "A Nonlinear Control Law for AMD with Stroke Limitation of the Moving Mass", Proc. of the 3rd Colloquium on Vibration Control, JSCE(in Japanese)

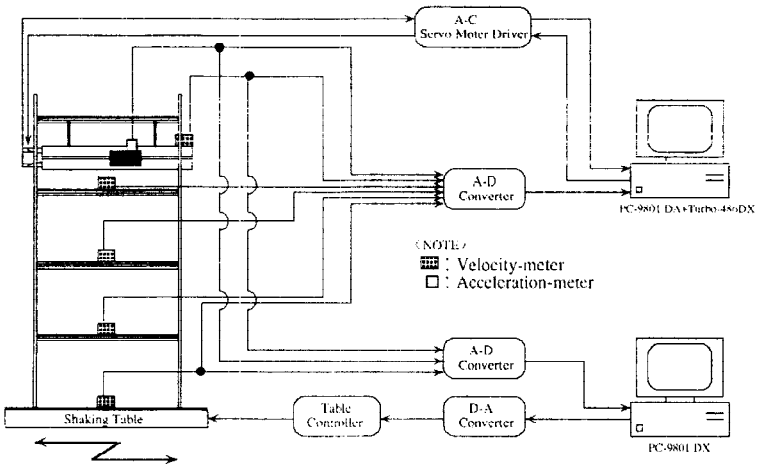

Fig.1 Experimental System for Control

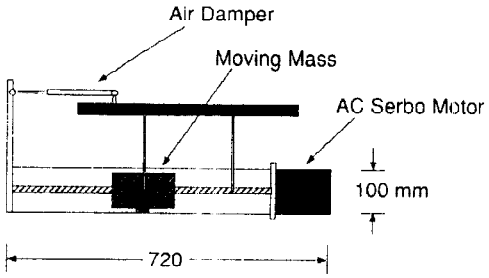

Fig.2 TMD and SOTMD

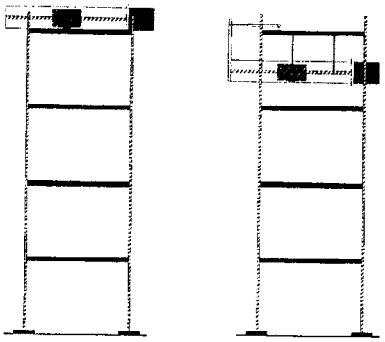

(a) AMD (b) TMD, SOTMD

Fig.3 Model with Control Devices

Table 1 Natural Period of the Model

Mode	Natural Period (sec)	Damping Ratio(%)	Participacion Factior
1	0.675(0.662)	0.39	(1.241)
2	0.225(0.229)	3.58	(0.333)
3	0.138(0.149)	4.41	(0.183)
4	- (0.122)	-	(-0.079)

( ) is Analytical Values

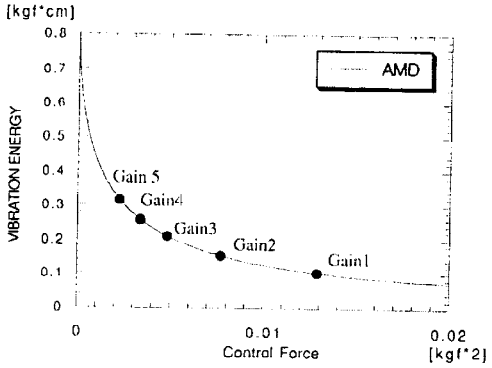

Fig.4 Trade-off Curves and Gains

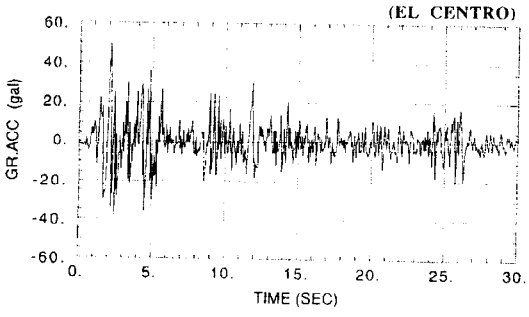

Fig.5 El Centro NS Acceleration Record (1940)

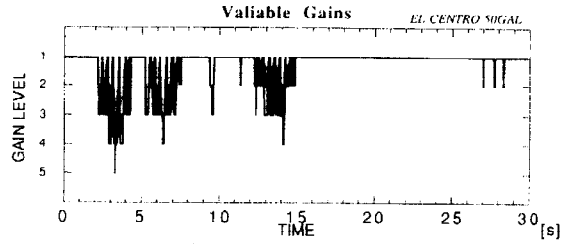

(a) Gain Level

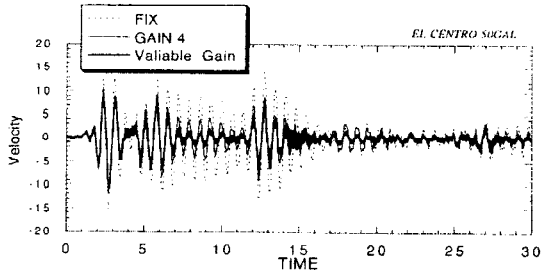

(b) Time History

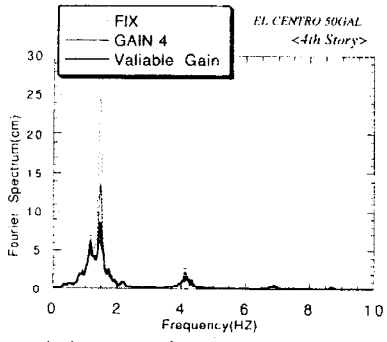

(c) Fourier Spectrum

Fig.6 Comparison of Response with AMD between Canstant Gain and Variable Gain

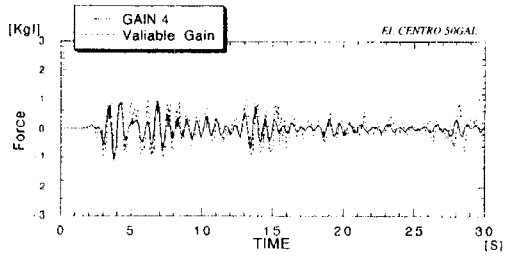

(a) Time History

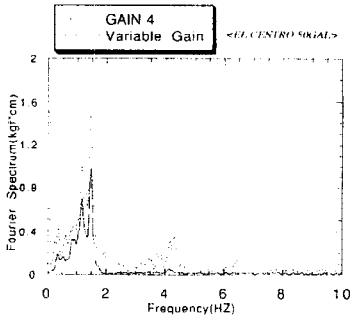

(b) Fourier Spectrum

Fig.7 Comparison of Control Force

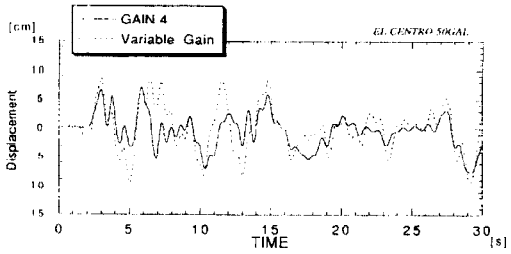

Fig.8 Comparison of Mass Displacement

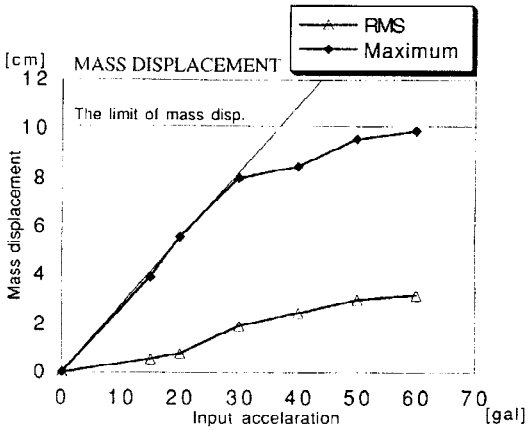

Fig.9 Mass Displacement

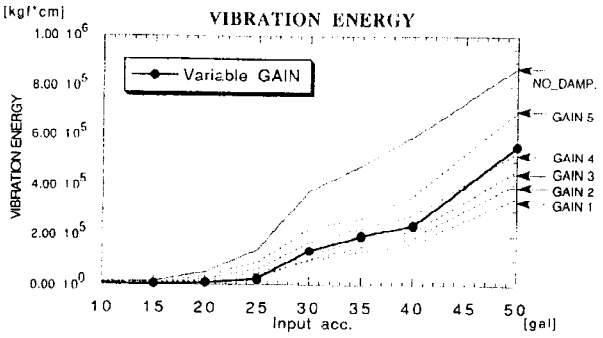

Fig.10 Vibration Energy

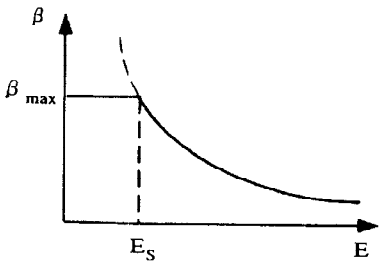

Fig.12 The Variable Gain with the Vibration Energy

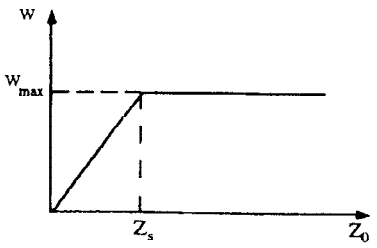

Fig.13 The Maximum Stroke of AMD with The Intensity of Excitation

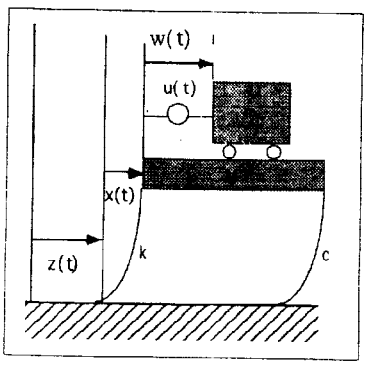

Fig.11 Notations of a Structure with AMD

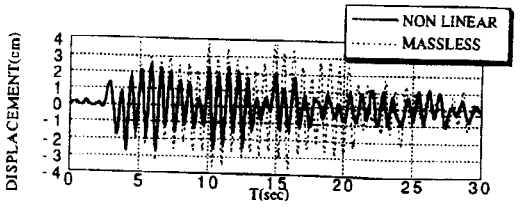

(a) Structural Displacement Response

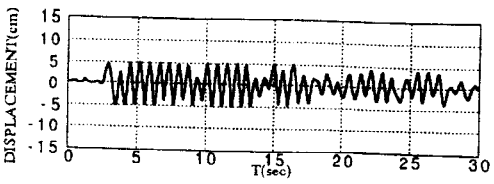

(b) Displacement Response of AMD

Fig.14 Earthquake Response with and without Control (α =10)

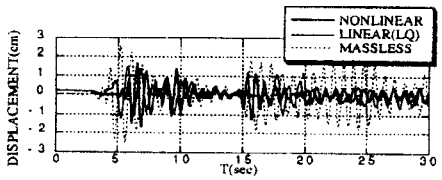

(a) Structural Response

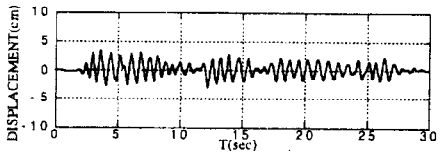

(b) Displacement of AMD (Nonlinear Control)

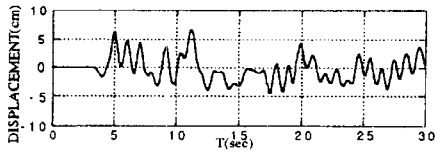

(c) Displacement of AMD (LQ Control)

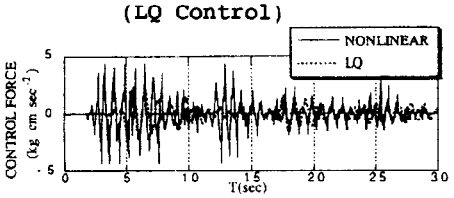

(d) Control Force

Fig.15 Expenrimental Results

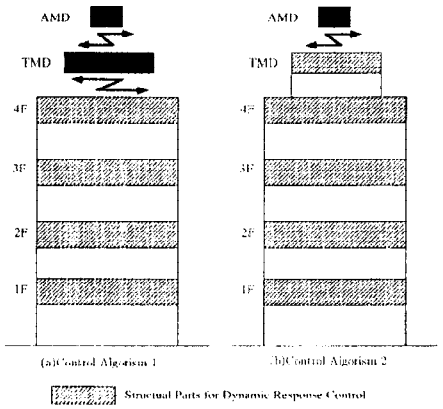

Fig.16 Control Algorithms

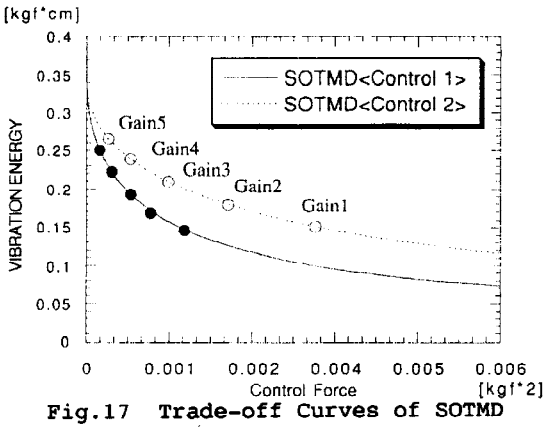

Fig.17 Trade-off Curves of SOTMD

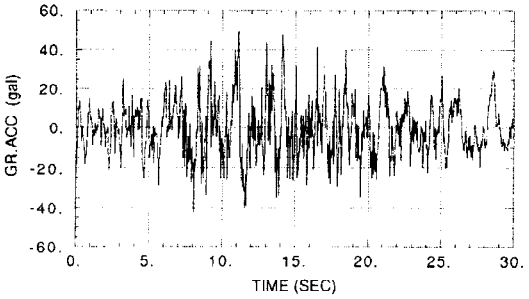

Fig.18 The Artificial Earthquake Motion for Soil II

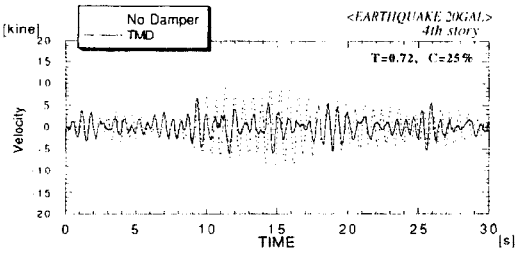

(a) TMD

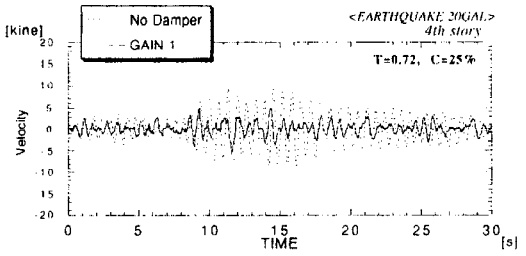

(b) SOTMD (Control 1)

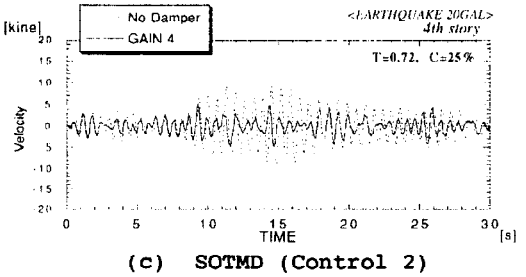

(c) SOTMD (Control 2)

Fig.19 Comparison of Time History Response

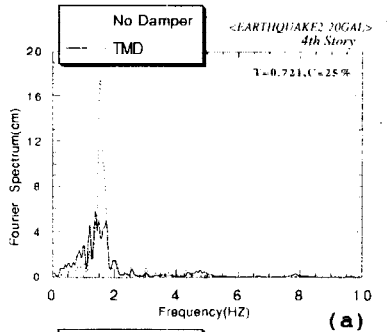

(a) TMD

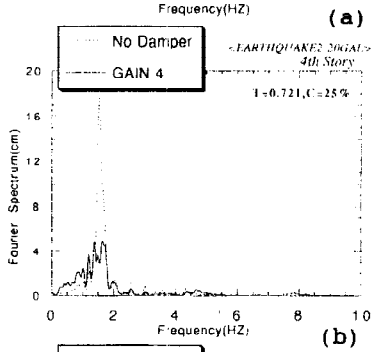

(b) SOTMD (Control 1)

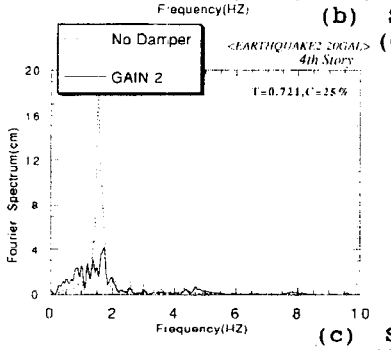

(c) SOTMD (Control 2)

Fig.20 Fourier Spectra of Response

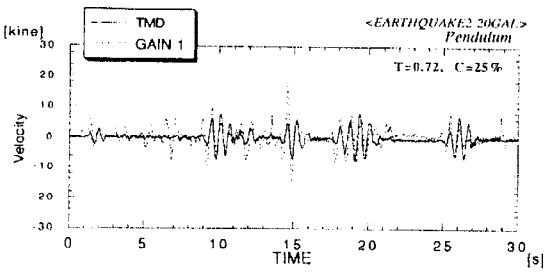

(a) SOTMD (Control 1)

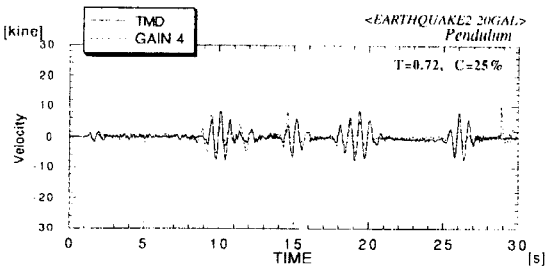

(b) SOTMD (Control 2)

Fig.21 Time History of SOTMD Velocity

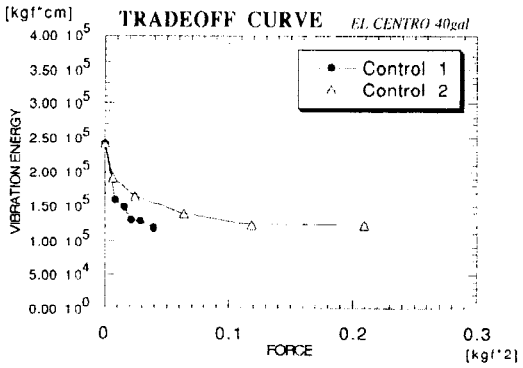

Fig.22 Trade-off Curves from Experiments

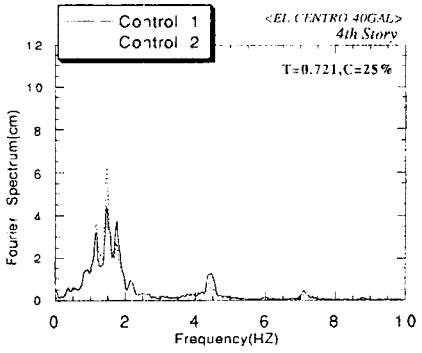

Fig.23 Comparison of Response between Control 1 and 2

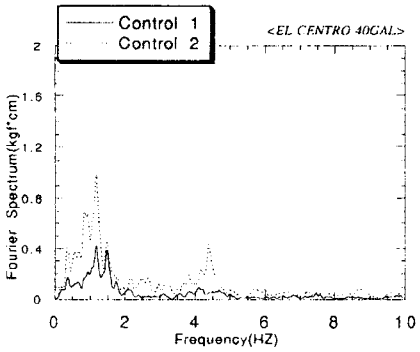

Fig.24 Comparison of Control Force between Control 1 and 2

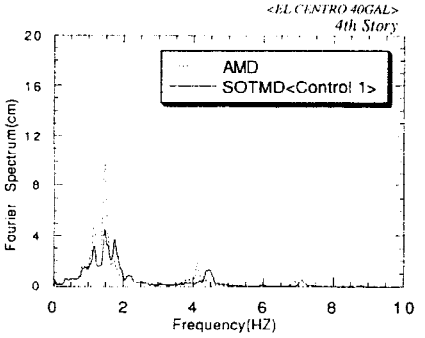

Fig.25 Comparison of Response between AMD and SOTMD

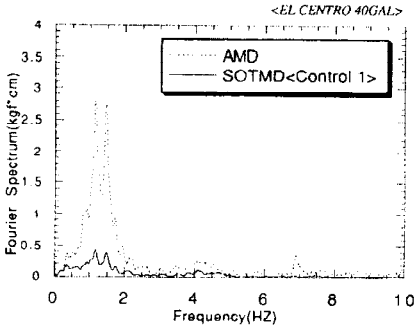

Fig.26 Comparison of Control Force between AMD and SOTMD